Seismic Three-Dimensional Stability of Concave Slopes by Lower Bound Limit Analysis

Faradjollah Askari

Assistant Professor, Geotechnical Engineering Research Center, International Institute of Earthquake Engineering and Seismology (IIEES), Iran, email: askari@iiees.ac.ir

ABSTRACT

This paper is devoted to present a method of three-dimensional stability analysis of concave slopes in plan view based on lower-bound theorem of the limit analysis approach in static and seismic cases. Slope stability problems are often analyzed two-dimensionally by conventional limit equilibrium method (LEM). Accuracy of LEM is often questioned due to the underlying assumptions that it makes, and at the same time, analyzing a 3D problem two-dimensionally may lead to significant differences in safety factors depending on the slope geometries. In this paper, the numerical linear finite element and the rigorous lower bound limit analysis method is used to produce some seismic stability dimensionless charts for three-dimensional (3D) homogeneous concave slopes. The charts can be used by practicing engineers as a convenient tool to estimate the stability for excavated or man-made slopes. The results obtained using this 3D method show that the stability of concave slopes increases as the relative curvature R/H and the relative width of slope decrease.

1. Introduction

Up to now, stability of slopes has been traditionally analyzed two-dimensionally by practitioners. During the past decades, some three-dimensional slope stability methods have been proposed. Most of these analyses have dealt with straight (in plan view) slopes with a planar surface. However, there are many concave slopes in plan view with non-planar surfaces. The influence of plan curvature on the stability of slopes has been investigated mainly by Giger and Krizek [1, 2], Leshchinsky et al [3], Leshchinsky and Baker [4], Baker and Leshchinsky [5], Xing [6], Michalowski [7], Farzaneh and Askari [8], and Ohlmacher [9] for some special cases. Giger and Krizek [1, 2] used the upper-bound theorem of limit analysis to study the stability of a vertical corner

cut subjected to a local load. They assumed a kinematically admissible collapse mechanism and, through a formal energy formulation, assessed the stability with respect to shear strength of soil. They presented a 3D analysis of slope stability based on the variational limiting equilibrium approach and proved that it can be considered as a rigorous upper bound in limit analysis. Leshchinsky and Baker [4] used a modified solution of the approach mentioned to study 3D end effects on stability of homogeneous slopes constrained in the third direction and applied it to investigate the stability of vertical corner cuts. Using a variational approach, Baker and Leshchinsky [5] discussed the stability of conical heaps formed by homogeneous soils. Xing [6] proposed a 3D stability

analysis for concave slopes in plan view using the equilibrium concept. Based on the limit equilibrium method, Michalowski [7] introduced a rigorous 3D approach in the strict framework of limit analysis for homogeneous and straight slopes. In his analysis, the geometry of slope and slip surface was unrestricted and both cohesive and frictional soils were included. Farzaneh and Askari [8] improved Michalowski's algorithm in the case of 3D homogeneous slopes and extended it to analyze the stability of nonhomogeneous slopes. Ohlmacher [9] investigated a case study including concave and concave slopes.

Ignoring the 3D effects when analyzing slopes can lead to unsafe answers. As an example, in the back analyses of shear strengths, neglecting the 3D effects will lead to values that are too high, and therefore affect any further stability assessments.

In this paper, finite element lower bounding method is used and 3D stability charts are presented, which may be used to evaluate the safety factor in seismic 3D concave slope stability problems.

2. Background

Idealizing the soil behavior as a perfectly plastic material obeying the associated flow rule, two plastic bounding theorems can be proved and used to obtain the lower and upper bounds of the limit load in limit analysis method. According to the upper bound theorem, if a set of external loads acts on a failure mechanism and the work done by the external loads in an increment of displacement equals the work done by the internal stresses, the external loads obtained are not lower than the true collapse loads. It is noted that the external loads are not necessarily in equilibrium with the internal stresses and the mechanism of failure is not necessarily the actual failure mechanism. By examining different mechanisms, the best (least) upper bound value may be found. The lower bound theorem states if an equilibrium distribution of stress covering the whole body can be found that balances a set of external loads on the stress boundary and is nowhere above the failure criterion of the material, the external loads are not higher than the true collapse loads. It is noted that in the lower bound theorem, the strain and displacements are not considered and that the state of stress is not necessarily the actual state of stress at collapse. By examining

different admissible states of stress, the best (highest) lower bound value may be found.

Limit theorems have not been applied to 3D slope stability problems as widely as they have been used in 2D problems. Currently, most slope stability evaluations based on the limit theorems such as Giger and Krizek [1, 2], Michalowski [7, 10], Donald and Chen [11], Chen et al [12, 13], Farzaneh and Askari [8, 14] and Viratjandr and Michalowski [15], have used the upper bound method alone. Michalowski [7], who investigated local footing load effects on the 3D slope stability, presented major contributions for upper bound 3D soil slope stability analysis.

Three-dimensional limit analysis applications has almost exclusively concentrated on the upper bound method because of the difficulties of constructing statically admissible stress fields analytically in 3D problems. The finite element lower bound limit analysis techniques developed by Lyamin and Sloan [16] and Krabbenhoft et al [17] provided a useful numerical method for dealing with complex problems (Appendix 1). The method was used in three-dimensional analyses of convex slopes by Askari et al [18] in static cases. This paper is devoted to use the linear finite element and an optimization approach to find the lower bound solutions in seismic 3D concave slope stability problems.

3. Formulation of the Problem

Suppose a body with volume V and surface area A, and t and q are the set of known and unknown tractions acting on the surface areas A_t and A_q respectively. Similarly, let g be the system of fixed and known body forces which act, respectively, on the volume V. Under these conditions, the objective of a lower bound calculation in a limit load problem (such as a bearing capacity problem) is to find a stress distribution that satisfies equilibrium throughout V, balances the prescribed tractions t on A_t and body forces on g, nowhere violates the yield criterion, and maximizes the integral:

$$Q = \int_{A_q} q \, dA \tag{1}$$

As will be shown later, the formulation can be easily rearranged to find the safety factor in a stability problem (such as slope stability problems).

This problem can be solved analytically for a few simple cases; however, the most appropriate method for this task in problems with complex geometries, inhomogeneous material properties, and complicated loading patterns may be considered the finite element method.

Formulation of the lower bound theorem in this problem leads to a constrained optimization problem of the form:

Maximize Objective Function

subject $\quad a_i(x) = 0 \qquad i \in I = \{1,...,m\}$

to $\qquad f_j(x) \le 0, \quad j \in J = \{1,...,r\}$ (2)

$\qquad x \in R^n$

where x is an n-dimensional vector of stress variables. The equalities defined by the functions a_i follow from the element equilibrium, discontinuity equilibrium, and boundary and loading conditions, while the inequalities defined by the functions f_j arise because of the yield constraints and the constraints on applied forces. Maximizing Objective Function leads to use an optimization approach.

In this paper, the nonlinear optimization based on a fast quasi-Newton method whose iteration count is largely independent of the mesh refinement, is selected for finding the maximum lower-bound solution of the safety factor of the slope, which satisfies the elements equilibrium, discontinuities equilibrium, and boundary and loading conditions.

The schematic geometry of the concave slope considered in this paper and the section of the slope at plane of symmetry are shown in Figure (1).

The global form of a typical element in present solution is shown in Figure (2). The stress variation between each two nodes of the element is assumed linear, thus this type of finite element is called Linear Finite Element. The following section gives a detailed description of the discretization procedure for the case of three-dimensional linear elements.

Unlike the usual form of the finite element method in which each node is unique to a particular element, multiple nodes can share the same coordinates, and statically admissible stress discontinuities are permitted at all inter-element boundaries.

Elements are organized from some prismatic units as shown in Figure (3). Each discussed unit is combined from three volumetric pyramid elements, shown in Figure (4).
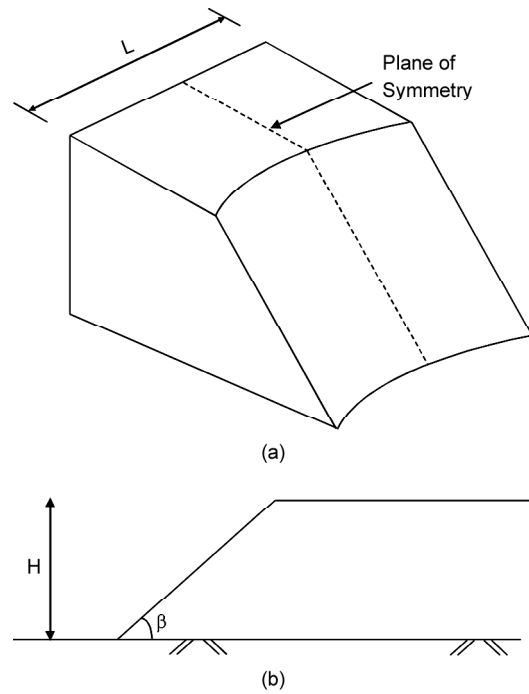
The global form of modeling consists of two

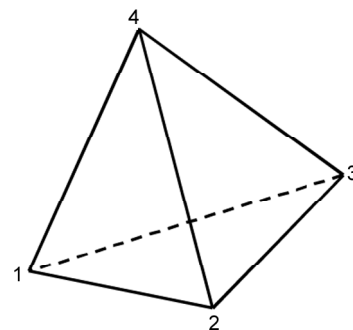**Figure 1.** (a) Schematic model of the concave slope analyzed (b) section at plane of symmetry.

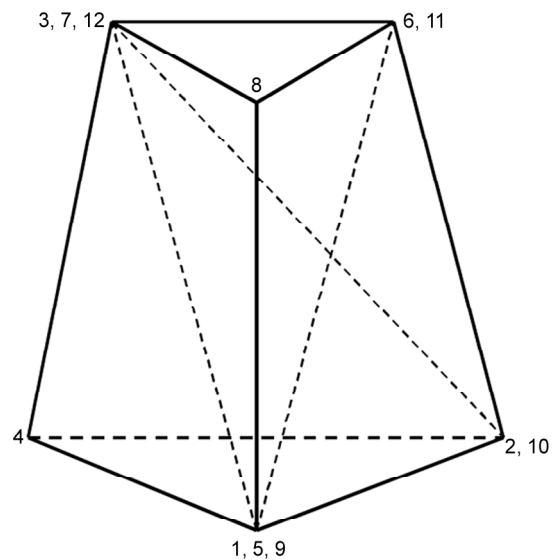**Figure 2.** Global form of a typical element [18].

Figure 3. Prismatic unit used for organizing the elements [18].

plans, one locates at the top and the other at the bottom of the model. Figure (5) shows the top and bottom plans of modeling. Between each pair of
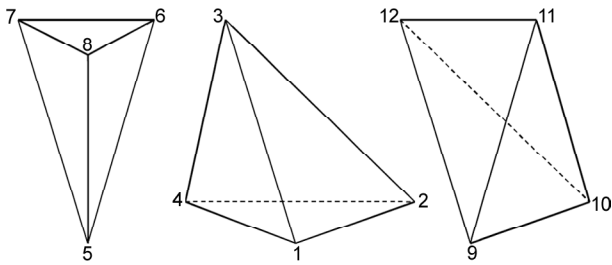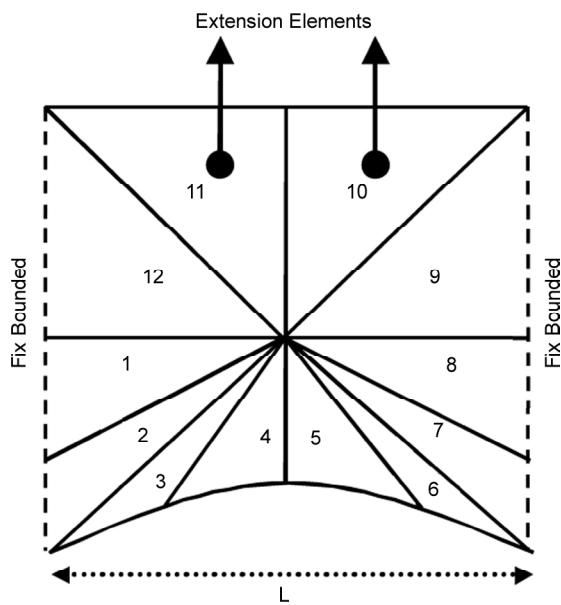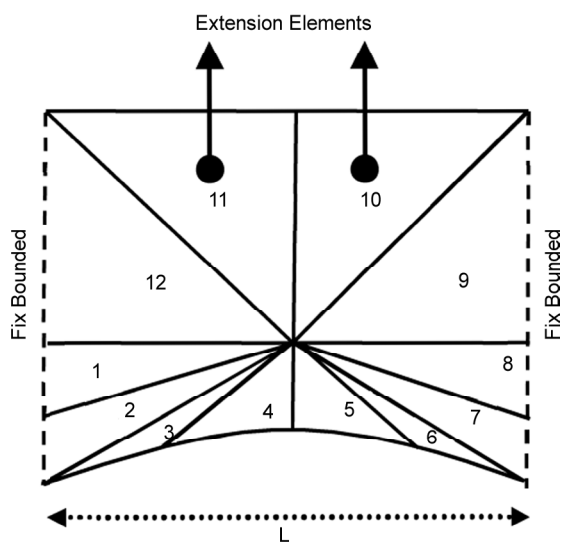

Figure 4. Elements used for Lower Bound Limit Analysis [18].

(a) Bottom Plan

(b) Top Plan

Figure 5. Bottom and top plans of modeling, extension of the stress fields into a semi-infinite domain.

slices in the plans (1 to 12), three elements in the form of a prismatic unit shown in Figure (3) are constituted. For higher slopes, various numbers of prismatic units are used in the height of the slopes.

The typical 3D slope model for the problem of this paper is shown in Figure (6). This model consists of 12 units and therefore 36 elements.
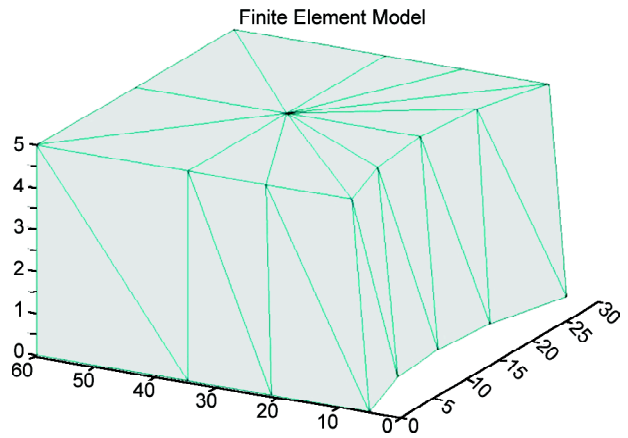

Figure 6. Typical 3D finite element model of the slope analyzed in this paper.

The extension elements may be used to extend the solution over a semi-infinite domain and therefore provide a complete statically admissible stress field for infinite half-space problems [16]. In fact, the extension elements referred to in Figure (5) can be used readily to extend the stress fields into a semi-infinite domain, which is discussed in Appendix 1. Because this paper is concerned mainly with the stability of finite slopes resting on a firm base, extension elements are needed only behind of slopes, shown in Figure (5).

4. Objective Function and Loading Constraints

The purpose of lower bound limit analysis is to find a statically admissible stress field, which maximizes the objective function with consideration of the combination of surface tractions and body forces of the problem. In the terminology of slope stability, safety factor is known as the objective function, since this is the quantity that is wanted to be maximized in lower bound case.

The general form of the yield condition for a perfectly plastic solid has the form:

$$f(\sigma_{ij}) \le 0 \qquad (3)$$

where f is a convex function of the stress components and material constants. The solution procedure presented later in this paper does not depend on a particular type of yield function, but does require it to be convex and smooth. Convexity is necessary to ensure that the solution obtained from the optimization process is the global optimum, and is actually guaranteed by the assumptions of perfect plasticity. Smoothness is essential because the solution algorithm needs to compute first and second derivatives of the yield function with respect to the unknown stresses. For yield functions, which have singularities in their derivatives, such as the Mohr-Coulomb criteria, it is necessary to adopt a smooth approximation of the original yield surface. A plot of this function in the meridional plane is shown in Figure (7).
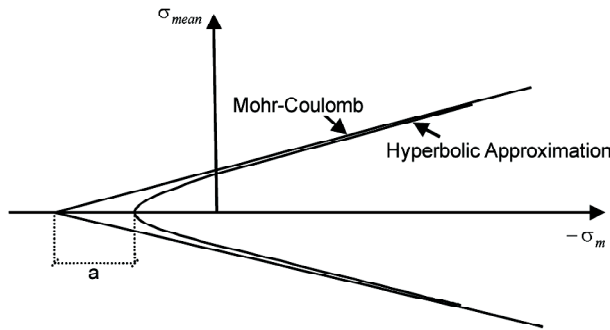

Figure 7. Hyperbolic approximation to Mohr-Coulomb yield function.

Defining tensile stresses as positive, the Mohr-Coulomb yield function may be written as:

$$f = (\sigma_1 - \sigma_2) + (\sigma_1 + \sigma_2)\sin\phi_d - 2c_d\cos\phi_d \qquad (4)$$

where the principal stresses are ordered so that $\sigma_1 > \sigma_2 > \sigma_3$ and c_d and ϕ_d are:

$$FS_c = c / c_d \qquad (5)$$

$$FS_\phi = \tan(\phi) / \tan(\phi_d) \qquad (6)$$

in which c and ϕ denote, respectively, the cohesion and friction angle of the soil. Assuming $FS = FS_c = FS_\phi$, the objective function define as maximizing the safety factor by satisfying the yield function. This implies that the stresses at all nodes in the finite element model must satisfy the yield condition.

Thus, in total, the yield conditions give rise to some non-linear inequality constraints on the nodal stresses.

Because each node is associated with a unique set of stress variables, it follows that each yield inequality is a function of an uncoupled set of stress variables σ_{ij}^l. Each admissible stress field has its own safety factor. Using an optimization method of nonlinear programming that is based on Newton's method the highest lower bound safety factor is attained. In this method, the non-linear equations at the current point k are linearized and the resulting system of linear equations is solved to obtain a new point $k + 1$. The process is repeated until the governing system of non-linear equations is satisfied. Thus, the highest lower bound safety factor of admissible stress fields is searched; this feature can be exploited to give a very efficient solution algorithm.

The typical lower bound finite element meshes and boundary conditions used to analyze the 3D slope problem are illustrated in Figure (6). The stability of homogeneous slopes is usually expressed in terms of two dimensionless stability numbers in the following form:

$$N_S = \gamma H F_S / c \qquad (7)$$

$$\lambda = N_S \tan\phi / F_S \qquad (8)$$

where N_S is the stability number, γ is the soil unit weight, H is the slope height, F_S is the safety factor of the slope. In addition, c and ϕ are known as the strength parameters of the material; c represents the cohesion and ϕ represents the angle of internal friction.

5. Comparison with Other Results

Increasing the number of elements in models increases the accuracy of the results; however, high number of elements leads to time-consuming runs. In order to select an optimum number of elements, some models were made and results by different number of elements were compared to make a decision on the number of elements to use and suitable time taken in each run.

For constant quantity of slope angle $\beta = 30$ and $\lambda = 2$, the results of some straight slopes for elements number 18, 36 and 72 are compared, shown in Figure (8). As it is seen, an increase in elements number results in decreasing the interspaces between lower bound solutions. It means that by increasing the number of elements, the accuracy of results is
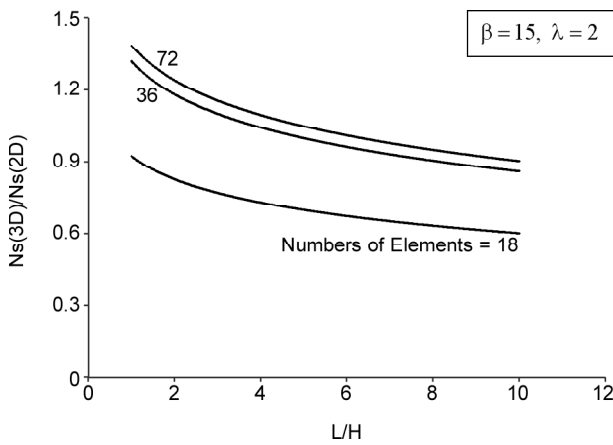
Figure 8. Effect of element numbers in accuracy of results.

increased, but its rate decreases, as Figure (8) shows. Therefore, it can be concluded that for higher number of elements, the difference between results can be connivance. In this paper, all numerical results are made of 36 elements because of low rate of variations afterwards.

For a validation, the results of the current approach can be compared with those of other investigators for straight slopes. Different methods have been proposed for 3D analysis of straight slopes by Baligh and Azzouz [19], Chen and Chameau [20], Ugai [21], and Leshchinsky and Baker [4]. Comparing the current results with most of these methods, a good agreement is found among them. Leshchinsky and Baker [4] extended a modified limit equilibrium solution of variational approach in 3D stability of slopes. Ugai [21] extended Baker variational limit equilibrium approach to 3D cohesive slopes.

Figure (9) shows the ratio F_{3D}/F_{2D} (F_{iD} is the safety factor in iD analysis) as a function of L/H
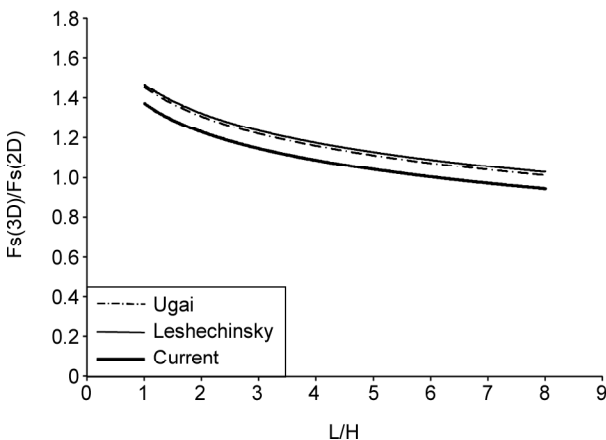

Figure 9. Comparison of the present results with those of Ugai [21] and Leshchonsky [4] in cohesive soils.

obtained by Ugai [21], Leshchinsky and Baker [4] and the present solution. As it is seen, the results of current solution underestimate in good accuracy.

6. Numerical Results

The analysis developed in this paper allows for calculations of three-dimensional safety factors and stability numbers in concave slopes, for which the failure mechanism is expected to pass through or above the toe, and for slopes with no pore-water pressure within the failure mechanism.

In Figures (10) to (13), stability diagrams for homogeneous concave slopes in plan view obtained from numerical lower bound analyses are displayed for slope angles (β) 45° and 90°, λ equal to 0 and 3 and seismic coefficients (k_h) ranging from 0 to 0.3. These diagrams demonstrate the stability for three ranges of the relative curvature radius of the slope in plan (R/H) for different L/H ratios (L and H are shown in Figure (1)). The stability numbers for 2D cases are obtained from bishop's simplified method. The relative width of the mechanism of failure, L/H, ranges from 2 to 10.

Although the diagrams are results of lower bound method, the true ratio of F_{3D}/F_{2D} has been investigated and identified to be bracketed by the numerical upper and lower bound analysis within a range of ±9% for all cases considered.

A comparison of the equivalent 2D and 3D cases can be made by investigating the factor of safety ratio F_{3D}/F_{2D} for the same slope angle (β), seismic coefficient (k_h), and slope height dimensionless parameters L/H and λ. The ratio F_{3D}/F_{2D} is simply equal to the ratio of the stability numbers $N_{s(3D)}/N_{s(2D)}$.

Following results can be obtained based on the diagrams shown in Figures (10) to (13):

ι Three-dimensional effects (the ratio $N_{s(3D)}/N_{s(2D)}$) decrease as the slope angle (β) and λ increase. The effect increases as the seismic coefficient (k_h) increases. In other words, 3D analyses are more important in cohesive soils with gentle slopes in seismic areas.

ι N_s decreases when L/H ratio increases. Therefore, using 2D solution is conservative for design of slopes. However, the solution may be non-conservative when determining strength parameters from a back analysis of a failed slope.
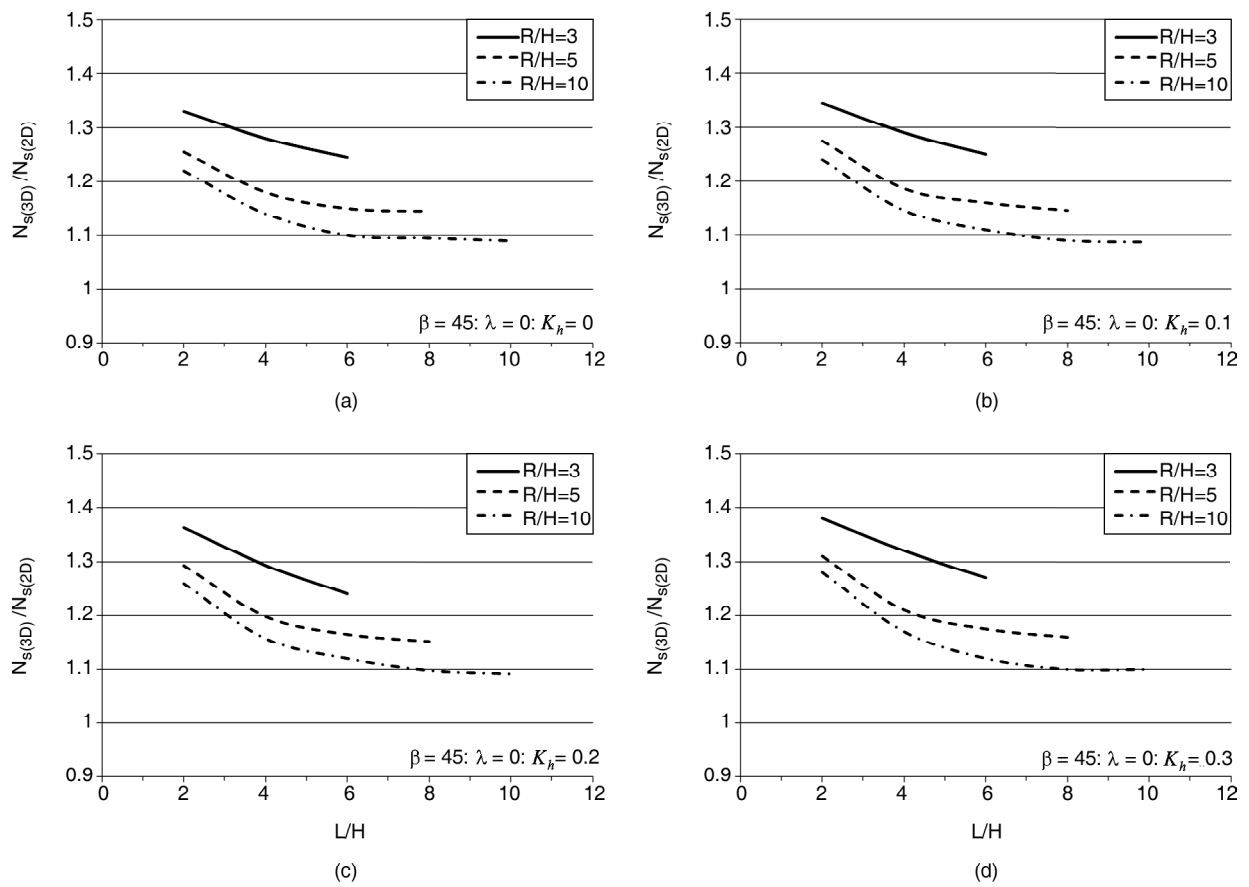
Figure 10. Seismic stability number ratios in different L/H ratios for β=45 and λ =0.
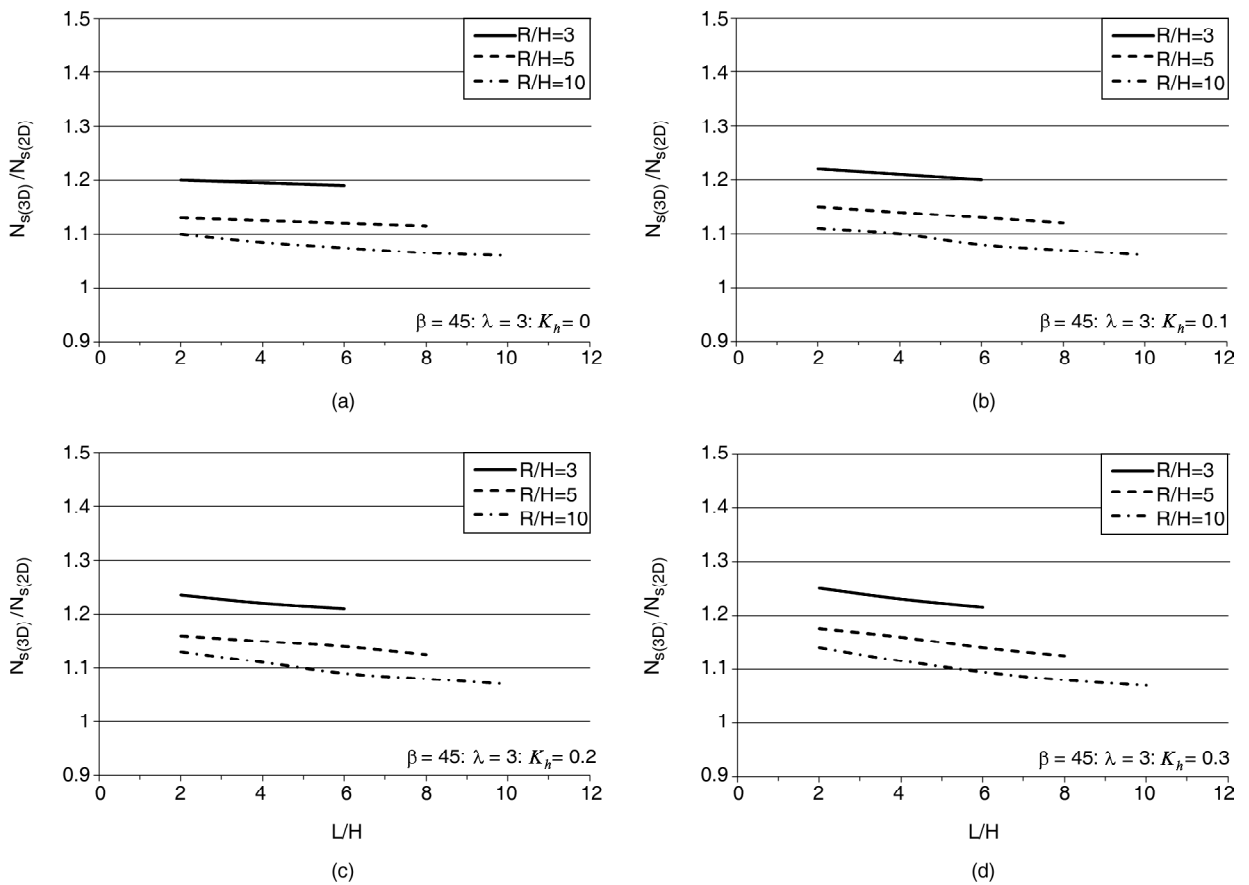

Figure 11. Seismic stability number ratios in different L/H ratios for β=45 and λ =3.
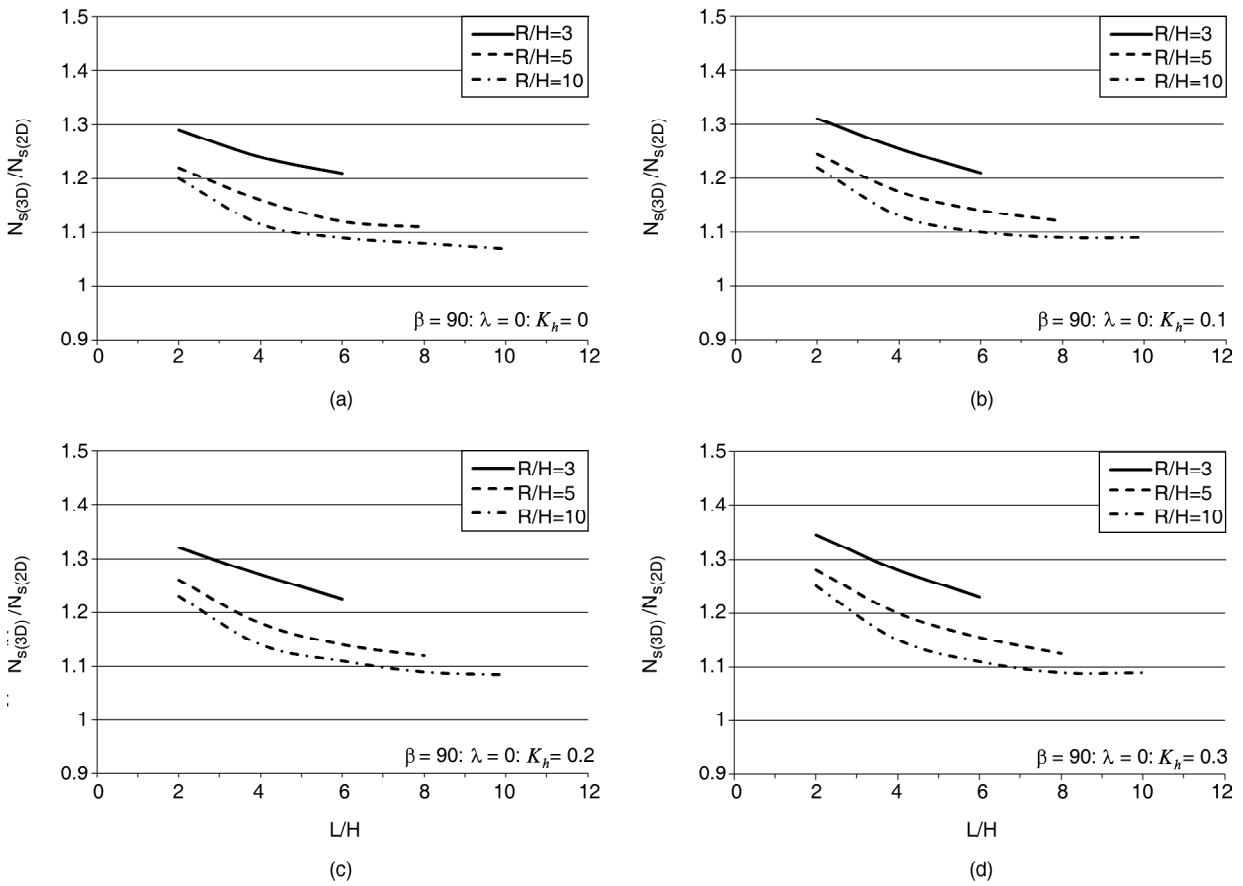
Figure 12. Seismic stability number ratios in different L/H ratios for β=90 and λ =0.
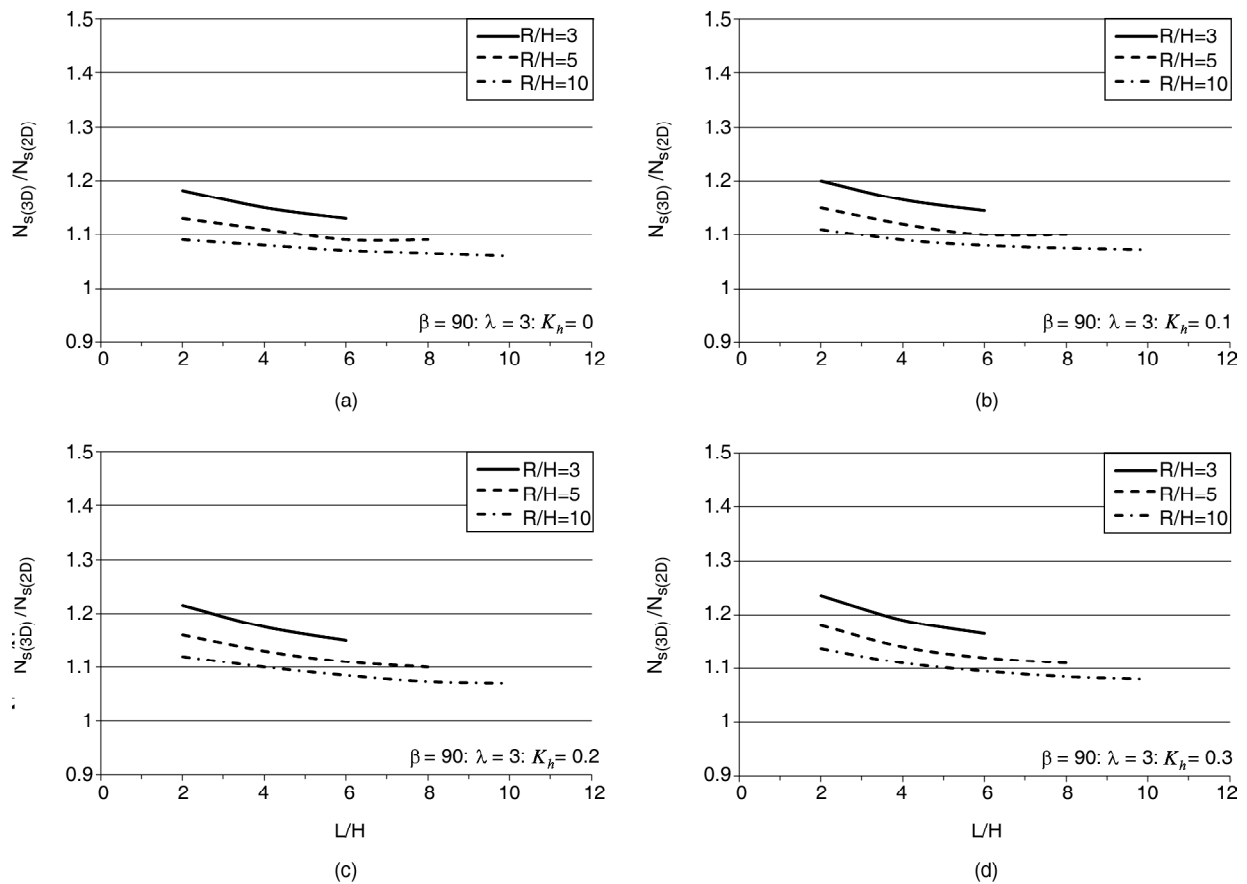

Figure 13. Seismic stability number ratios in different L/H ratios for β=90 and λ =3.

ı For a given β, λ and k_h, N_s achieve the minimum value when *L/H* goes to infinite. This implies that the 3D factor of safety will reduce with increasing *L/H* ratio. As is known, the plane strain analysis does not consider the resistance provided by the two lateral ends of the slip surface. The boundary resistance from these two ends can be seen as 3D end boundary effect, which makes the slope more stable. While increasing the *L/H* ratio, the relative contributions of resistances provided by lateral ends decrease, which means that 3D end boundary effect reduces. Therefore, using 2D stability numbers will lead to a more conservative slope design.

ı For a given concave slope, the stability number increases as the ratio *R/H* decreases. In other words, concave slopes in plan view are more stable than straight ones.

7. Conclusions

A method was presented for the evaluation of the three-dimensional stability of concave slopes in plan view based on Lower-bound theorem of the limit analysis approach subjected to seismic excitation. Slope stability problems are often analyzed two dimensionally by conventional limit equilibrium method (LEM). Accuracy of LEM is often questioned due to the underlying assumptions that it makes and at the same time, analyze a 3D problem two dimensionally may lead to significant differences in safety factors depending on the slope geometries.

Limit analysis is a powerful tool for evaluation of the stability of slopes. The analysis presented includes 3D and seismic effects of concave slopes. Seismic effects are approximated as pseudo static loadings and it does not account for the periodicity during seismic shaking.

The charts produced for homogeneous cohesive slopes can be used by practicing engineers as a convenient tool to estimate the three-dimensional effects in stability of concave slopes.

Based on the results presented, the smaller the curvature radius of the slope (*R/H*), the higher the stability of concave slope in plan view is. It should be mentioned that with decreasing λ and increasing seismic coefficient (k_h), three-dimensional effects are more significant. In other words, the effect of curvature of the slope is more important in cohesive soils with gentle slopes in seismic areas.

References

1. Giger, M.W. and Krizek, R.J. (1975) Stability analysis of vertical cut with variable corner angle. *Soils and Foundations*, **15**(2), 63-71.

2. Giger, M.W. Krizek, R.J. (1976) Stability of vertical corner cut with concentrated surcharge load. *Journal of the Geotechnical Engineering Division*, **102**(1), 31-40.

3. Leshchinsky, D., Baker, R., and Silver, M.L. (1985) Three-dimensional analysis of slope stability. *International Journal for Numerical and Analytical Methods in Geomechanics*, **9**(3), 199-223.

4. Leshchinsky, D. and Baker, R. (1986) Three-dimensional slope stability: end effects. *Soils and Foundations*, **26**(4), 98-110.

5. Baker, R. and Leshchinsky, D. (1987) Stability analysis of conical heaps. *Soils and Foundations*, **27**(4), 99-110.

6. Xing, Z. (1988) Three-dimensional stability analysis of concave slopes in plan view. *Journal of Geotechnical Engineering*, **114**(6), 658-671.

7. Michalowski, R.L. (1989) Three-dimensional analysis of locally loaded slopes. *Geotechnique*, **39**(1), 27-38.

8. Farzaneh, O. and Askari, F. (2003) Three-dimensional analysis of nonhomogeneous slopes. *Journal of Geotechnical and Geoenvironmental Engineering*, **129**(2), 137-145.

9. Ohlmacher, G.C. (2007) Plan curvature and landslide probability in regions dominated by earth flows and earth slides. *Engineering Geology*, **91**(2), 117-134.

10. Michalowski, R.L. (2002) Stability charts for uniform slopes. *Journal of Geotechnical and Geoenvironmental Engineering*, **128**(4), 351-355.

11. Donald, I.B. and Chen, Z. (1997) Slope stability analysis by the upper bound approach: fundamentals and methods. *Canadian Geotechnical Journal*, **34**(6), 853-862.

12. Chen, Z., Wang, X., Haberfield, C., Yin, J.H., and Wang, Y. (2001) A three-dimensional slope stability analysis method using the upper bound theorem: Part I: theory and methods. *International Journal of Rock Mechanics and Mining Sciences*, **38**(3), 369-378.

13. Chen, J., Yin, J.H., and Lee, C.F. (2003) Upper bound limit analysis of slope stability using rigid finite elements and nonlinear programming. *Canadian Geotechnical Journal*, **40**(4), 742-752.

14. Farzaneh, O., Askari, F., and Ganjian, N. (2008) Three-dimensional stability analysis of convex slopes in plan view. *Journal of Geotechnical and Geoenvironmental Engineering*, **134**(8), 1192-1200.

15. Viratjandr, C. and Michalowski, R.L. (2006) Limit analysis of submerged slopes subjected to water drawdown. *Canadian Geotechnical Journal*, **43**(8), 802-814.

16. Lyamin, A.V. and Sloan, S.W. (2002) Lower bound limit analysis using non-linear program ming. *International Journal for Numerical Methods in Engineering*, **55**(5), 573-611.

17. Krabbenhoft, K., Lyamin, A.V., Hjiaj, M., and Sloan, S.W. (2005) A new discontinuous upper bound limit analysis formulation. *International Journal for Numerical Methods in Engineering*, **63**(7), 1069-1088.

18. Askari, F., Totonchi, A., and Farzane, O. (2012) 3D stability analysis of convexslopes in plan view using linear finite element and lower bound method. *International Journal of Civil Engineering*, **10**(2), 112-123.

19. Baligh, M.M. and Azzouz, A.S. (1975) End effects on stability of cohesive slopes. *Journal of the Geotechnical Engineering Division*, **101**(11), 1105-1117.

20. Chen, R.H. and Chameau, J.L. (1983) Three-dimensional limit equilibrium analysis of slopes. Geotechnique, **33**(1), 31-40.

21. Ugai, K. (1985) Three-dimensional stability analysis of vertical cohesive slopes. *Soils and Foundations*, **25**(3), 41-48.

Appendix

A.1. Linear Finite Element Formulations

As mentioned in the paper, the finite element formulation used is similar to those of Lyamin and Sloan [16]; however, in this study, the types of elements are different and the formulations are applied in seismic condition. Formulations are explained in more detail in reference [18]; however, a summary is presented in this Appendix.

The stresses, together with the body force components h_i, which act on a unit volume of material, are taken as the problem variables. The vector of unknowns for an element e is denoted by x_e and is written as:

$$x^e = \left\{ \{\sigma_{ij}^l\}^T, ..., \{\sigma_{ij}^{D+1}\}^T, \{h_i\}^T \right\}^T,$$
$$i = 1, ..., D; \ j = i, ..., D \tag{A1}$$

where $\{\sigma_{ij}^l\}$ denotes the stresses at node l and $\{h_i\}$ denotes the elemental body forces. The variation of the stresses throughout each element may be written conveniently as:

$$\sigma = \sum_1^4 N_l \sigma^l \tag{A2}$$

where N_l denotes the linear shape functions. The latter can be expressed as:

$$N_l = \frac{1}{|C|} \sum_0^3 (-1)^{l+k+1} \left| C_{(l)(k)} \right| x_k \tag{A3}$$

where x_k denotes the coordinates of the point at which the shape functions are to be computed (with the convention that $x_0 = 1$), C is a 4×4 matrix formed from the element nodal coordinates according to:

$$C = \begin{bmatrix} 1 & x_1^1 & x_2^1 & x_3^1 \\ 1 & x_1^2 & x_2^2 & x_3^2 \\ 1 & x_1^3 & x_2^3 & x_3^3 \\ 1 & x_1^4 & x_2^4 & x_3^4 \end{bmatrix} \tag{A4}$$

and $C_{(l)(k)}$ is a 3×3 submatrix of C obtained by deleting the lth row and the kth column of C. In above expressions, the superscripts are row numbers,

correspond to the local node number of the element, while the subscripts are the column numbers, and designate the coordinate index. Elements in the first terms of Eq. (A2) can be written in the more compact form:

$$N_l = \sum_0^3 a_{lk} x_k \qquad (A5)$$

$$a_{lk} = (-1)^{l+k+1} \frac{\left| C_{(l)(k)} \right|}{|C|} \qquad (A6)$$

A.2. Element Equilibrium

To generate a statically admissible stress field, the stresses throughout each element must obey the equilibrium equations:

$$\frac{\partial \sigma_{ij}}{\partial x_j} + h_i = -g_i, \quad i = 1, 2, 3 \qquad (A7)$$

where σ_{ij} are Cartesian stress components, defined with respect to the axes x_j, and g_i and h_i are, respectively, prescribed and unknown body forces acting on a unit volume of material within the element. Writing the governing equations in terms of stress vector, which reduces the number of unknowns, Eq. (A5) becomes in following matrix notation:

$$A_{equil} x^e = b_{equil} \qquad (A8)$$

in which A_{equil} is coefficients matrix of equilibrium and b_{equil} is constant matrix of equilibrium. Thus, in total, the equilibrium condition generates three equality constraints on the element's variables in three-dimensional modeling.

A.3. Discontinuity Equilibrium

To incorporate statically admissible discontinuities at inter-element boundaries, it is necessary to enforce additional constraints on the nodal stresses. A statically admissible discontinuity requires continuity of the shear and normal components but permits jumps in the tangential stress. Since the stresses vary linearly along each element side, static admissibility is guaranteed if the normal and shear stresses are forced to be equal at each pair of adjacent nodes on an inter-element boundary.

In the previous section, the components of the stress tensor were defined with respect to the rectangular Cartesian system with axes x_j, $j = 1, 2, 3$.

In addition to this global coordinate system, let us define a local system of Cartesian co-ordinates x'_k, $k = 1, 2, 3$, with the same origin but oriented differently, and consider the stress components in this new reference system. Assuming these two coordinate systems are related by the linear transformation:

$$x'_k = \beta_{kj} x_j, \quad k = 1, 2, 3 \qquad (A9)$$

where β_{kj} are the direction cosines of the x'_k-axes with respect to the x_j-axes, then the tractions acting on a surface element, whose normal is parallel to one of the axes x'_k, are given by the vector t^k with components:

$$t_i^k = \sigma_{ij} \beta_{kj} \qquad (A10)$$

The corresponding transformation law for the stress components is:

$$\sigma'_{km} = \sigma_{ij} \beta_{ki} \beta_{mj} \qquad (A11)$$

Using the definition of the stress vector, and assuming that the normal to the discontinuity plane is parallel to the axis x'_l, Eq. (A9) may be written as:

$$A_{disc} x^e = b_{disc} \qquad (12)$$

in which A_{disc} is coefficients matrix and b_{disc} is constant matrix. Hence, the equilibrium condition for each discontinuity generates nine equality constraints on the nodal stresses.

A.4. Boundary Conditions

Consider a distribution of prescribed surface tractions t_p, $p \in P$ where P is a set of N_p prescribed components, which act over part of the boundary area A_t. For the case of a linear finite element, where the tractions are specified in terms of global coordinates over the linearized boundary area A_t^d, we can cast the stress boundary conditions for every node l as:

$$\sigma_{ip}^l \beta_{ki}^l = t_p^l \qquad (A13)$$

Assuming the local coordinate system is chosen with x'_l parallel to the surface normal at node l, this type of stress boundary condition gives rise to the constraints:

$$A_{bound} x^e = b_{bound} \qquad (A14)$$

in which A_{disc} is coefficients matrix and b_{disc} is

constant matrix. Thus, every node, which is subject to prescribed surface tractions, generates a maximum of three equality constraints on the unknown stresses.

A.5. Assembly of Constraint Equations

All of the necessary steps to formulate the lower bound theorem as an optimization problem have now been covered. The only step remaining is to assemble the constraint matrices and objective function coefficients for the overall mesh. Using mentioned equations, the various equality constraints may be assembled to give the overall equality constraint matrix according to:

$$A_{global} = \sum_1^E A_{equil} + \sum_1^{Ds} A_{disc} + \sum_1^{Bn} A_{Bound} \quad (A15)$$

where E is the total number of elements, Ds is the total number of discontinuities, Bn is the total number of boundary nodes, which are subject to prescribed surface tractions. Similarly, the corresponding right-hand side vector b is assembled according to:

$$b_{global} = \sum_1^E b_{equil} + \sum_1^{Ds} b_{disc} + \sum_1^{Bn} b_{Bound} \quad (A16)$$

When the stress field is modeled using linear finite elements, the objective function and equality constraints are linear in the unknowns, with the only non-linearity arising from the yield inequalities. Thus, the problem of finding a statically admissible stress field that maximizes the collapse load may be stated as:

Maximize $\quad C^T x$

subject to $\quad Ax = b$

$$f_j(x) \leq 0, \quad j \in R^n \quad (A17)$$

$$x \in R^n$$

where c is a vector of objective function coefficients of length n, A is an $m \times n$ matrix of equality constraint coefficients, $f_j(x)$ are yield functions and other convex inequality constraints and x is a vector of length n which is to be determined.

A.6. Extension of Stress Field into Semi-Infinite Domain

When the lower bound method described previously is applied to problems with semi-infinite domains, only part of the body is discretized. This means that the optimized stress field does not

necessarily satisfy equilibrium, the stress boundary conditions and the yield criterion throughout the entire domain; and therefore, it cannot be used to infer a rigorous lower bound on the collapse load. Although this type of solution, which is known as a partial stress field, may actually furnish a good estimate of the true collapse load, a fully rigorous lower bound can be obtained only by extending the stress field over the semi-infinite domain in such a way that all the conditions of the lower bound theorem are fulfilled. This process is often difficult, especially for cases involving irregular boundary shapes, and is frequently omitted in hand calculations. To resolve this situation, some extension elements, which are deployed around the periphery of the mesh, are used. These are constructed so that they extend the stress field beyond the limits of the grid in such a way that it is statically admissible.

A D-dimensional extension element is much like a regular lower bound finite element in that the stress field is defined by the stresses at $D+1$ nodes and the body forces are assumed to be constant. Indeed, as with any lower bound element, the stresses must satisfy the equilibrium, stress boundary and yield conditions. Consider the 2D case, where a linear expansion is used to model the stresses across and outside a three-noded extension element. Provided the equilibrium and stress boundary conditions are satisfied within the triangle, then they are automatically satisfied for any point p outside the triangle. This implies that all extension elements are subject to the same equilibrium and stress boundary constraints as regular elements. For D-dimensional geometries, a maximum of D different types of extension elements are required. Although they are restricted to certain types of yield criteria, extension elements are attractive because they guarantee that the solution obtained is a rigorous lower bound.
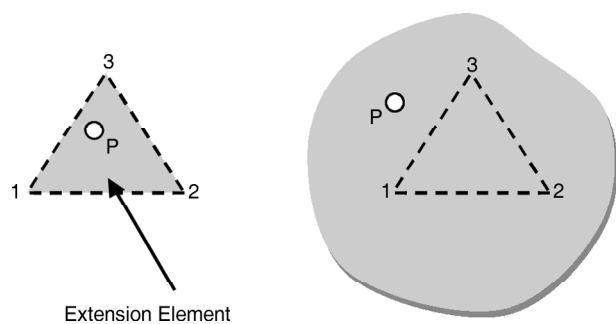

Figure A.1. Approximation of stress field inside and outside the extension element.